ELSEVIER

Chemical Engineering Journal 66 (1997) 51–56

CHEMICAL ENGINEERING JOURNAL

Effect of ageing on a steam reforming catalyst

Haitham al-Qahtani

Chemical Engineering Department, University of Bahrain, Isa Town, P.O. Box 32038, State of Bahrain

Received 1 March 1996; accepted 17 June 1996

Abstract

The present study investigates the effect of ageing on the performance of an industrial steam reforming catalyst. The surface and the composition of the catalyst were analyzed by using scanning electron microscopy and dispersive X-ray spectrometry methods. From the results, it was found that the changes in the surface properties and the chemical content of the catalyst reduced the catalyst activity. The reduction is attributed to the continuous increase in the furnace temperature which was required in order to maintain the same level of hydrocarbon conversion.

Keywords: Steam reforming; Catalytic ageing; Synthesis gas

1. Introduction

The steam reforming process is used to convert hydrocarbons into hydrogen and carbon monoxide. The process is the major industrial source of carbon monoxide and hydrogen. It is utilized heavily by the petrochemical, refinery, steel production industries and other hydrogenation processes. The demand for the synthesis gas will increase in the future [1].

Since the reaction is endothermic, both heat and catalyst are applied to enhance the conversion. Table 1 shows the effect of temperature on the equilibrium constant for the methane stream reforming reaction [2]

$$CH_4 + H_2O \rightarrow CO + 3H_2 \quad (1)$$

Feedstock selection for the steam reforming process is determined by the type of available hydrocarbon. In Japan and India, for instance, naphtha is the major feedstock, while in West Europe and Arabian Gulf countries natural gas is the more suitable feedstock.

For the catalyst type, it was found that elements of group VIII (Fe, Co, Ni, Rd, Ru, Pd, Os, Ir and Pt) were active for the steam reforming reaction [3]. Nickel is the major metal used in the steam reforming catalyst. Large catalyst size is preferred due to the high flow rate in the usual application. The catalyst support should be strong enough to withstand the operating conditions. Also, it must be able to disperse the metal catalyst and to allow an access for the species to approach the surface. It was found that support could enhance the adsorption of steam and influence the reaction order [4].

PII S1385-8947(96)03149-1

Table 1
Variation of equilibrium constant with temperature of methane steam reforming

Temp. (K)	Equilibrium constant K
273	6.00×10^{-31}
373	2.70×10^{-20}
473	4.90×10^{-14}
573	6.80×10^{-10}
673	6.20×10^{-7}
773	1.02×10^{-4}
873	5.40×10^{-3}
973	1.30×10^{-1}
1073	1.76
1173	15.33
1273	95.50

The selected catalyst should meet the following characteristics [2].

- Approach to equilibrium. The catalyst should be active enough to convert the reactants into products close to the equilibrium conversion.
- Constant pressure drop. It is necessary to maintain equal distribution of flow in the blank of the tubes of the reactor. Degradation of the catalyst results in partial or total blockage which leads to the development of hot spots damaging the tubes.

The mechanism of a methane steam reforming reaction over nickel and iron catalyst was studied by many researchers [5–8]. The mechanism may be represented by the following reactions:

$$CH_4 \rightarrow C(ads) + 2H_2 \quad (2)$$

$$H_2O \rightarrow O(ads) + H_2 \quad (3)$$

$$C(ads) + O(ads) \rightarrow CO \quad (4)$$

The objective of the present study was to investigate the effect of the operating time on the catalyst performance. To conduct the study, steam to carbon ratios, product concentrations, exit temperature, pressure drop, synthesis gas selectivity and yield were monitored on a weekly basis from when the catalyst was installed in February 1992, in an industrial reactor, until it was removed from the production line in September 1995. In addition scanning electron microscopy (SEM) and dispersive X-ray spectrometry (EDS) for both the used and unused catalysts were used to investigate the catalyst surface and composition.

2. Process description

The feedstock was a natural gas consisting of about 80% methane, whose composition is shown in Table 2. The natural gas stream was mixed with a recovered gaseous stream coming from the hydrogenation process (composition is given in Table 3) and then desulfurized.

After leaving the desulfurization process, the gas stream was mixed with superheated steam at ratios of 2.40 to 2.60 (steam/natural gas). The mixture then entered the steam reforming reactor. The reactor consisted of seven vertical banks each consisting of 45 tubes. Each tube was filled with ceramic solid cylindrical catalyst. The dimensions of the catalyst cylinders were 19 mm o.d. and 10 mm i.d., and 18 mm in length respectively. The composition of the catalyst is shown in Table 4.

Table 2
Natural gas chemical composition

Component	mol.%
Methane	79.05
Ethane	1.52
Propane	0.36
n-Butane	0.10
Iso-butane	0.07
n-Pentane	0.04
Iso-pentane	0.05
Cyclopentane	0.01
Hexane	0.02
Nitrogen	12.12
CO_2	6.00
H_2S	0.05

Table 3
Hydrogenation feed composition

Composition	mol.%
CH_4	6.27
CO	2.08
CO_2	1.50
HS_2	77.43
N_2	12.70
Ar	0.02

Table 4
Chemical properties of the catalyst

Component	
Nickel oxide	15–17%
Carrier	$MgAl_2O_4$
SiO_2	<0.2%
S	<50 ppm
Cl	<25 ppm

The product leaving the reactor consisted of CO_2, CO, H_2, H_2O and CH_4.

3. Analysis

In order to analyze the performance of the catalyst during the continuous operation, the following parameters were measured on a weekly basis.

- Inlet molar flow rate of the feed and steam mixture before the inlet of the reformer.
- Gas composition of the inlet and outlet gas mixtures of the reformer.
- Inlet and exit temperatures.
- Synthesis gas selectivity and yield.
- Deviation from equilibrium temperature.

The synthesis gas selectivity and yield are defined according to the following:

$$\text{CO selectivity} = \frac{(CO)_{exit} - (CO)_{inlet}}{[(CH_4) + (2C_2H_6) + (3C_3H_8) + (4C_4H_{10})]_{inlet} - (CH_4)_{exit}} \quad (5)$$

$$H_2 \text{ selectivity} = \frac{(H_2)_{exit} - (H_2)_{inlet}}{[(2CH_4) + (3C_2H_6) + (4C_3H_8) + (5C_4H_{10})]_{inlet} - (2CH_4)_{exit}} \quad (6)$$

$$\text{CO yield} = \frac{(CO)_{exit} - (CO)_{inlet}}{[(CH_4) + (2C_2H_6) + (3C_3H_8) + (4C_4H_{10})]_{inlet}} \quad (7)$$

$$H_2 \text{ yield} = \frac{(H_2)_{exit} - (H_2)_{inlet}}{[(2CH_4) + (3C_2H_6) + (4C_3H_8) + (5C_4H_{10}) + (H_2)]_{inlet}} \quad (8)$$

To calculate the variation between the ideal temperature and the real one, equilibrium constant comparisons were con-

ducted. The equilibrium constant K_{eq} is calculated from the equation

$$K_{eq} = P_{CO} \times P_{H_2}^3 / P_{CH_4} \times P_{H_2O}$$

where P_i is the product partial pressure.

From the catalyst manual, the corresponding thermodynamic temperature can be found based on the calculated K_{eq}. This temperature will be used to determine the equilibrium approach value. The equilibrium approach is defined as the difference between the value of the exiting temperature which was measured at the reformer outlet and the value of the thermodynamic temperature which was determined from the calculated K_{eq}.

4. Sample analysis methods

The catalyst beads were 16 mm long cylinders with diameters of 20 mm. Several beads from used and unused catalysts were selected and they were fractured along the axis to ravel the inner surface of the holes. The samples were mounted on the specimen mount with the help of carbon point. The samples were initially observed in the uncoated condition and EDS analysis was performed. Subsequently the samples were coated with a thin layer of gold using a spatter coater in order to reduce the charging effect. A 20 kV electron beam was used for both observation and EDS analysis.

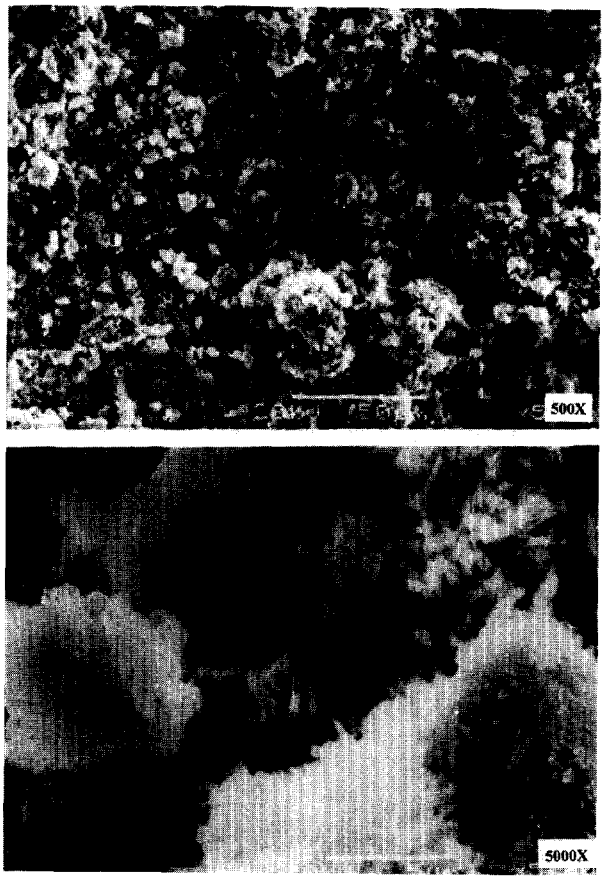

Fig. 1. SEM pictures showing the catalyst surface of an unused catalyst at 500× and 5000× (23 mm:50 μm).

5. Results and discussion

The unused catalyst showed fine particles on the sample surface characterized with high porosity. Needle-shaped nickel oxide particles could be seen dispersed over an alumina and magnesium oxide base. Fig. 1 shows the micrographs of a typical area taken at magnifications of 500× and 5000×. Similar observations were achieved with different samples of unused catalyst. Fig. 2 shows the EDS spectra of the unused catalyst obtained from the 500× area.

The distribution of various elements which was obtained by an X-ray map of the 5000× micrograph area is shown in Fig. 3.

The used sample surface shows lower porosity and nickel oxide particles seem to have conglomerated. Micrographs taken at magnifications of 500× and 5000× are shown in Fig. 4.

Fig. 5 shows the EDS spectra of the used catalyst obtained from the area of the 500× micrograph. The relative weight percentages of elements were calculated using ZAF correction for used and unused catalysts (see Table 5).

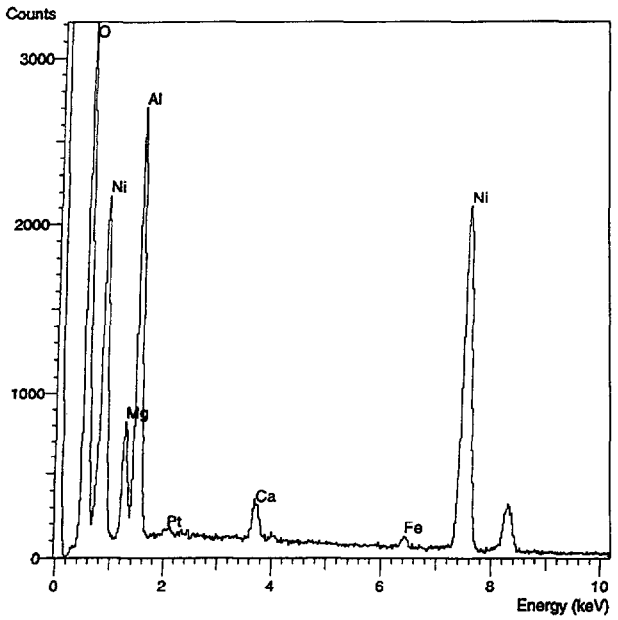

Fig. 2. EDS spectra of an unused catalyst at 500× area.

Table 5
Relative weight percentages of elements of unused and used catalysis

Element	wt.% (unused)	wt.% (used)
O	39.40	49.97
Mg	3.50	9.83
AL	14.19	24.56
Si	0.39	1.19
Ca	1.19	0.48
Fe	0.69	0.25
Ni	40.22	14.00
Pt	0.43	–

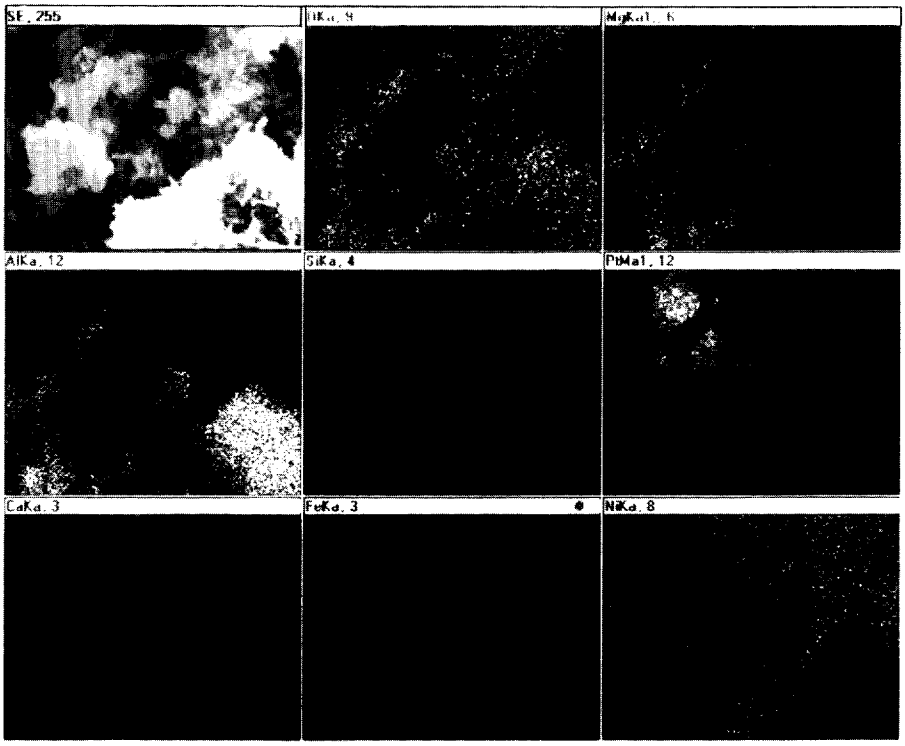

Fig. 3. X-ray map of the 5 000× micrograph area of an unused catalyst.

Fig. 4. SEM pictures showing the surface of a used catalyst at 500× and 5000× (23 mm:50 μm).

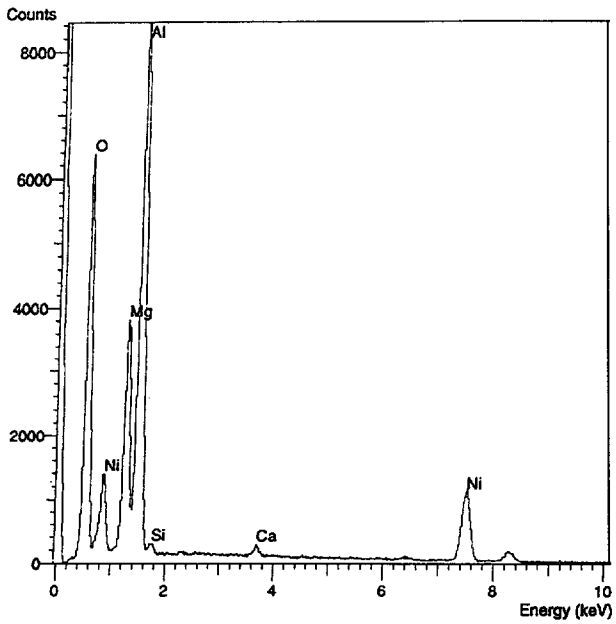

Fig. 5. EDS spectra of a used catalyst at 500× area and the analysis results of the spectrum.

Fig. 6 shows the distribution of the elements which was obtained by an X-ray map of the 5000× micrograph area of the used catalyst.

Comparing the EDS results and the relative weight of used and unused catalysts, the nickel oxide content had been reduced significantly and platinum was absent in the used catalyst sample.

No further analysis was conducted to investigate the reasons for the reduction in the Ni weight percentages nor the

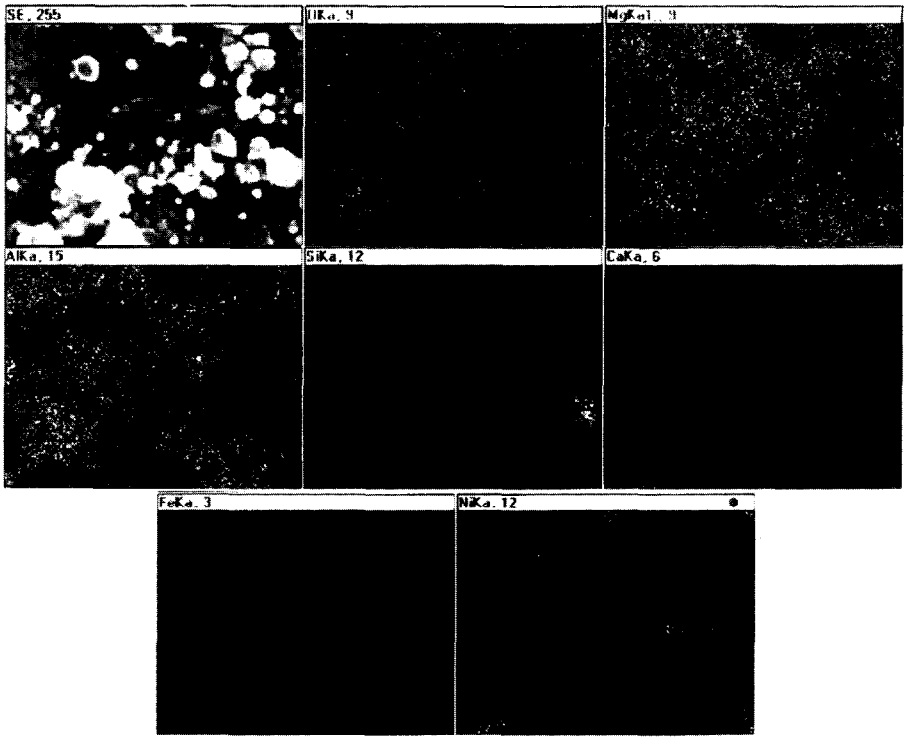

Fig. 6. X-ray map of the 5 000× micrograph area of a used catalyst.

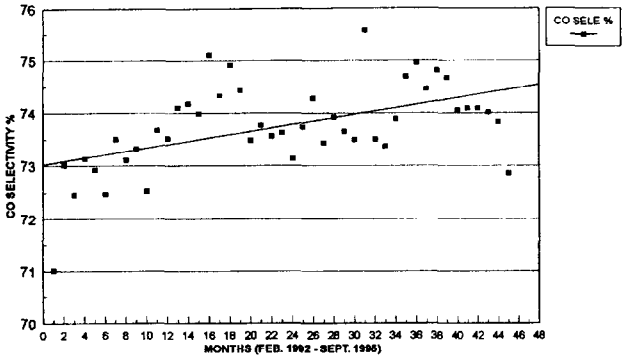

Fig. 7. Selectivity variation of CO.

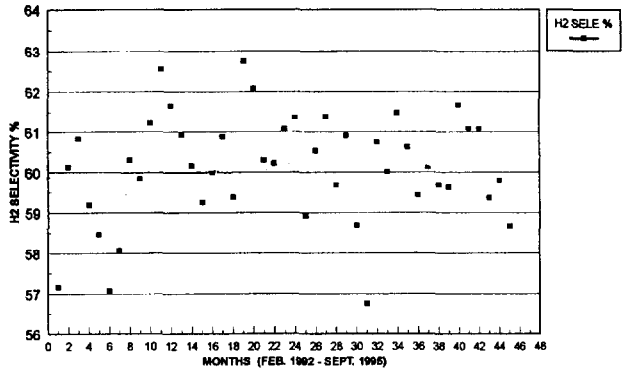

Fig. 8. Selectivity variation of H_2.

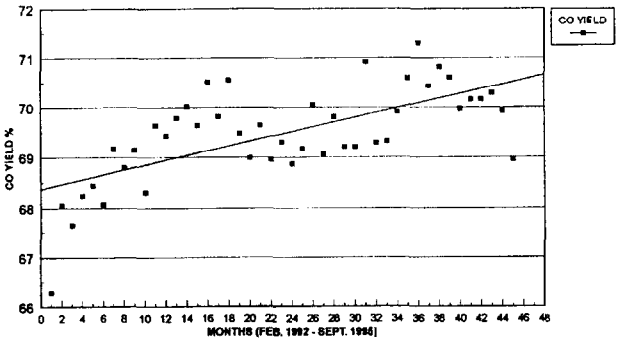

Fig. 9. Yield variation of CO.

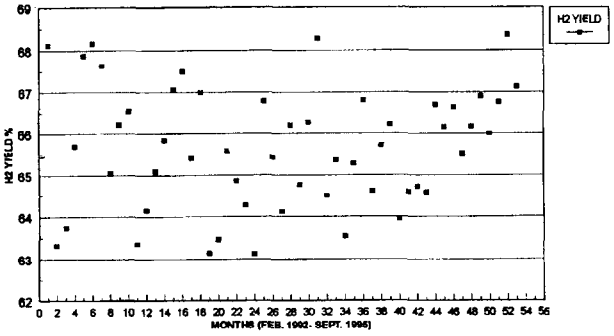

Fig. 10. Yield variation of H_2.

disappearance of the platinum. However, comparing the weight percentages of unused and used catalysts, Ni aluminate formation was not likely to occur since the weight percentage of the alumina element had increased as can be seen in the used catalyst. Volatilization of nickel in the form of nickel carbonyl was more likely to occur.

The CO selectivity and yield were increased with time, however no clear trends could be drawn from the H_2 selectivity and yield as shown in Figs. 7–10. The increment in the

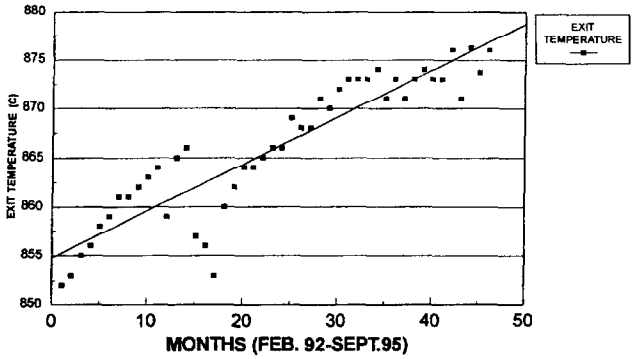

Fig. 11. Variation of exit temperature with time.

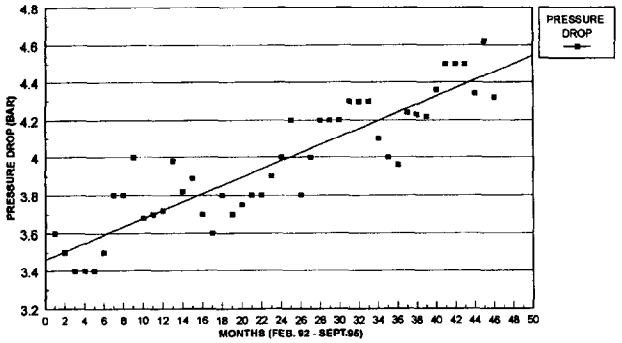

Fig. 12. Variation of pressure drop with time.

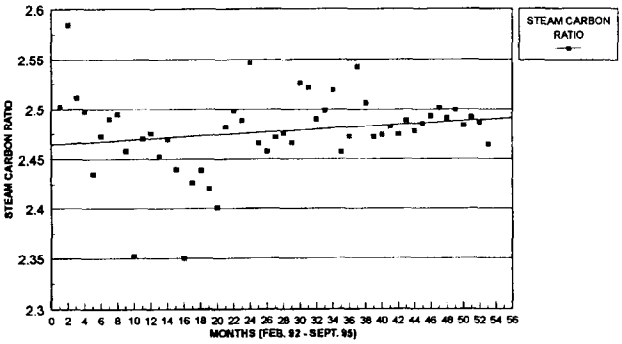

Fig. 13. Variation of steam carbon ratios with time.

CO selectivity and yield might be due to the increment in the temperature.

As shown in Fig. 11, the exit temperature increased with time and a similar increase to the pressure drop occurred (see Fig. 12). The steam carbon ratios were also increased slightly as shown in Fig. 13 where the equilibrium approach as shown in Fig. 14 was increased from negative values to positive ones.

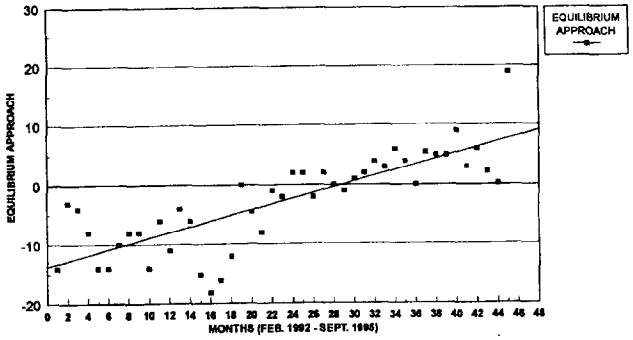

Fig. 14. Variation of equilibrium approach with time.

During the operation of the process, methane conversion was maintained higher than 99%. To maintain high conversion, a gradual increase in the temperature was required in order to compensate the reduction in the catalyst activity. The temperature in the reformer was increased from 850 up to 877 °C. Any further increase was not recommended due to the limitation in the maximum reactor temperature of the tubes at 880 °C. This was one of the factors which necessitated the removal of the catalyst from the reactor. The degradation in catalyst performance could also be seen from the increment in the pressure drop which indicated physical alteration of the catalysts resulting in blocking of the void spaces.

6. Conclusion

The effect of ageing on the steam reforming catalyst performance was found to reduce the porosity and the nickel content. These reductions deactivated the catalyst which was indicated by the increment in the operating temperatures, pressure drop and equilibrium approach.

References

[1] M. Twigg, *Catalytic Handbook*, Ch. 9, Wolfe, 1988.
[2] J. Rostrup-Nielsen, *Catalysis Science and Technology*, Volume 5, Springer–Verlag, 1984.
[3] D. Grenoble, *J. Catal., 51* (1978) 203.
[4] J. Rostrup-Nielsen, *J. Catal., 31* (1973) 173.
[5] I. Bodrove, L. Apel'baum and M. Temkin, *Katal, 5* (1964) 696.
[6] D. Allen, E. Gerharrd and J. Linkins, *Ind. Eng. Process Des. Dev., 14* (1975) 605.
[7] P. Munster and H. Grabe, *Ber. Bunsenges., Phys. Chem., 84* (1980) 1068.
[8] H. Al-Qahtani, D. Eng and M. Storkides, *Energy Fuels, 7* (1993) 495.